Novel diagnostic biomarkers for Alzheimer's disease in human tear fluid

Min Seok Baek

Department of Medicine

The Graduate School, Yonsei University

Novel diagnostic biomarkers for Alzheimer's disease in human tear fluid

Min Seok Baek

Department of Medicine

The Graduate School, Yonsei University

Novel diagnostic biomarkers for Alzheimer's disease in human tear fluid

Directed by Professor Chul Hyoung Lyoo

The Doctoral Dissertation
submitted to the Department of Medicine
the Graduate School of Yonsei University
in partial fulfillment of the requirements for the degree of
Doctor of Philosophy

Min Seok Baek

December 2021

ACKNOWLEDGEMENTS

I was able to finish this thesis thanks to the amazing energy of my inspiring mentor and supervisor, Professor Chul Hyoung Lyoo, whose kind and patient tutelage gave me the strength to reach the finish line. Through Professor Lyoo's constant guidance, I am always learning and growing.

I am also deeply grateful for the opportunity to have worked with Professors Young Hoon Ryu, Joong-Seok Kim, Hanna Cho, and Joon-Kyung Sung. Their diligence impacted my own and I thank each of them for all the great things that they have done for me.

I would like to extend special thanks to Professors Yong Woo Ji, Jae Hun Jung, and Hyung Keun Lee. Without their support, I could not have completed this thesis.

This manuscript is dedicated to my dear wife and my beautiful daughters, who always support me.

<TABLE OF CONTENTS>

LIST OF FIGURES

LIST OF TABLES

ABSTRACT

Novel diagnostic biomarkers for Alzheimer's disease in human tear fluid

Min Seok Baek

Department of Medicine
The Graduate School, Yonsei University

(Directed by Professor Lyoo Chul Hyoung)

Background: Cerebrospinal fluid (CSF) and positron emission tomography (PET) biomarkers are widely used as pathological biomarkers of Alzheimer's disease (AD). However, their use for population screening is restricted owing to their high cost and invasiveness. We investigated alterations in the tear proteins of patients with AD and mild cognitive impairment (MCI) using a proteomics approach.

Methods: We conducted tear proteome profiling using tandem-mass-tag labeling and liquid chromatography-mass spectrometry/mass spectrometry analysis in a global profiling cohort, with 42 participants including cognitively unimpaired (CU) individuals, and patients with amyloid-β (Aβ)-positive MCI (MCI+) and Aβ-positive AD (AD+). Eight differentially expressed proteins commonly expressed in MCI+ and AD+ were individually measured using parallel reaction monitoring from 103 participants in an individual analysis cohort. We performed logistic regression and receiver operating characteristic curve analysis between diagnostic groups, and a

correlation analysis using imaging biomarkers for regional Aβ, tau, and cortical volumes.

Results: We identified 3,350 tear proteins and selected eight candidate biomarkers from among 22 proteins quantifiable within an individual tear fluid sample. Of those, lipocalin 1 (LCN1), plastin-2 (LCP1), prolactin-inducible protein (PIP), secretoglobin family 2A member 1 (SCGB2A1), secretoglobin family 1D Member 1 (SCGB1D1), and glutamine synthetase (GLUL) showed areas under the curve (AUCs) ranging from 0.67 to 0.86 for discriminating AD+ from CU. The composite of biomarkers showed an AUC of more than 0.8 in discriminating MCI+ and AD+ from CU, and MCI+ from AD+. GLUL was positively associated with cortical Aβ burden, while LCN1 and LCP1 showed negative associations with Aβ and tau burden.

Conclusion: Tear fluid biomarkers have a predictive and discriminative role in the diagnosis of MCI and AD, and these biomarkers reflect underlying pathologic changes in AD.

Key words: Alzheimer's disease; mild cognitive impairment; tear fluid; proteomics; biomarker

Novel diagnostic biomarkers for Alzheimer's disease in human tear fluid

Min Seok Baek

Department of Medicine
The Graduate School, Yonsei University

(Directed by Professor Lyoo Chul Hyoung)

I. INTRODUCTION

Alzheimer's disease (AD) is characterized by the presence of two major pathological features: amyloid-β (Aβ) and tau burden in the cerebral cortex.[1] Postmortem studies have demonstrated that Aβ and tau pathology accumulate in stereotypical spatial patterns throughout the disease course.[2] In addition to the major pathological proteins, recent imaging and genetic studies have found that additional mechanisms such as inflammation, neurovascular disruption, and membrane dysregulation are involved in the pathogenesis of AD.[3, 4]

Currently, the most well-established AD pathological biomarkers include those found in cerebrospinal fluid (CSF) and positron emission tomography (PET) studies.[5] However, clinically these fall short of the criteria necessary for large-scale population screening because these modalities are expensive, require repeated exposure to radiation, or are too invasive.[6] To overcome these limitations, the search for effective AD biomarkers has expanded to the screening of biofluids including blood and tear fluid.[7]

Human tear fluid is a biological mixture containing high concentrations of proteins/peptides and metabolites, which are secreted by the lacrimal gland (LG) and ocular surface cells with rich innervation and vascularization.[8] The tear proteomic profile has provided biomarkers for ocular diseases including dry eye, glaucoma, and age-related macular degeneration.[9, 10] Furthermore, because there is an overlap between the tear proteome and plasma proteome, tear fluid may be a good source of non-invasive biomarkers, allowing the observation of systemic responses.[8] Previous research has identified protein alterations in tear fluid associated with systemic diseases such as Sjogren syndrome.[11] Nevertheless, studies on tear biomarkers for AD are limited and lack well-organized design with advanced analysis.

In this study, to identify novel AD diagnostic biomarkers and quantify targetable proteins, we applied a comprehensive proteomics approach using small volumes of tear fluid from cognitively unimpaired (CU) individuals, and patients with amyloid-β (Aβ)-positive mild cognitive impairment (MCI+) and Aβ-positive AD (AD+). Statistical modeling was applied to distinguish Aβ-positive mild cognitive impairment (MCI+), and Aβ-positive AD (AD+)

patients from cognitively unimpaired (CU) individuals. Finally, a correlation analysis was performed between individual tear fluid biomarkers and neuroimaging biomarkers reflecting Aβ and tau burden, and cortical volume in AD.

II. MATERIALS AND METHODS

1. Participants and study design

This study recruited participants for two separate cohorts from the Memory Disorder Clinic of Gangnam Severance Hospital. In the global profiling cohort, 42 participants [12 CU, 15 MCI+, and 15 AD+] were enrolled from July 2018 to December 2018; and for the individual analysis cohort, 103 participants [30 CU, 32 MCI+, and 41 AD+] were enrolled from July 2018 to April 2019. Four participants [3 CU, and 1 MCI+] in the global profiling cohort and nine participants [4 CU, 4 MCI+, and 1 AD+] in the individual analysis cohort refused APOE genotyping. Participants in both cohorts underwent the neuropsychological test battery, genotyping for apolipoprotein E (APOE), ^{18}F-florbetaben and ^{18}F-flortaucipir PET scans, and brain magnetic resonance (MR) imaging. Enrolled patients with AD fulfilled the National Institute on Aging Alzheimer's Association's (NIA-AA) diagnostic criteria for probable AD dementia with evidence of AD pathophysiological process. MCI patients fulfilled the NIA-AA criteria for MCI due to AD with intermediate or high likelihood.[12] CU participants had normal performance on baseline

neuropsychological tests and no abnormalities in brain MR imaging. A validated visual assessment method for ^{18}F-florbetaben PET was used to determine Aβ positivity.[13] A detailed study flow is summarized in Figure 1.

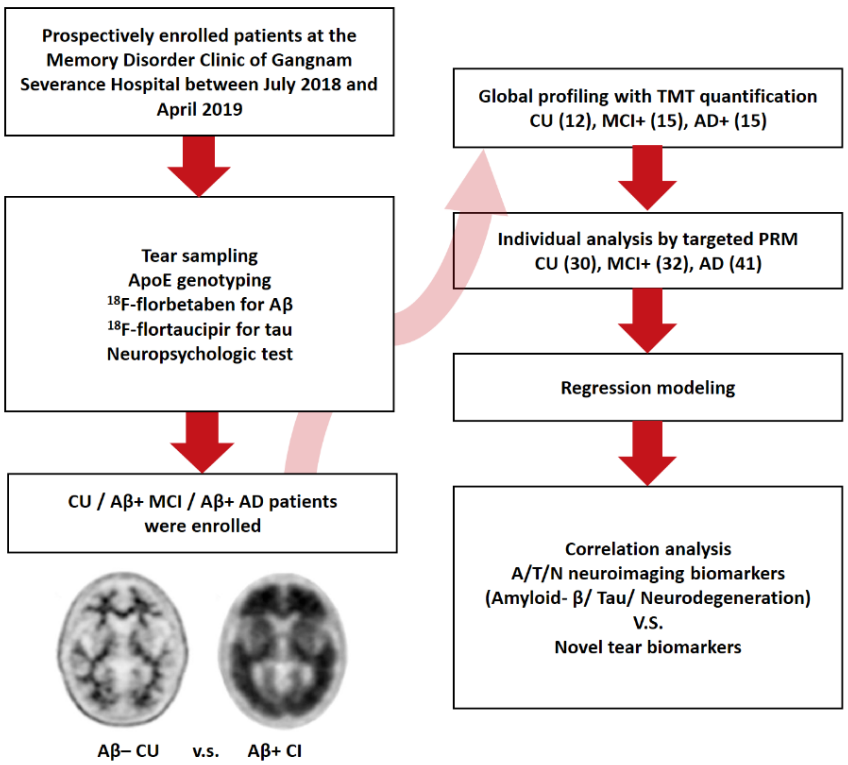

Figure 1. Overall workflow of the study

2. Tear sampling

A bonded 2.0 × 10 mm polyester fiber rod (TRANSORB® WICKS, FILTRONA, Richmond, VA, USA) was used to collect tear a fluid sample

from each participant, following a previously reported method.[9] In brief, for each participant, a polyester wick was applied to the tear meniscus of the lower lid margin, then it was removed and placed into a 1.5 ml Eppendorf tube, and stored at -70 °C until mass spectrophotometric assay was performed. This study was approved by the Institutional Review Board of Gangnam Severance Hospital (#3-2018-0156), and written informed consent was obtained from all participants and/or their legal guardians.

3. Quantitative global profiling and data processing

Proteins (100 μg) from pooled tear fluids were divided into two tubes as duplicates and digested into peptides by in-solution digestion. Each tube of tear peptide was labeled with TMT isobaric mass tagging reagent. The chemically tagged samples were pooled in one tube and peptide separation was carried out using high-pH reverse-phase liquid chromatography fractionation using the Q Exactive Orbitrap Hybrid Mass Spectrometer coupled with the nanoAQUITY UPLC system (Waters, CA, USA). Full mass spectrometry data were acquired with a scan range of 400–2,000 Th, at a resolution of 70,000 at m/z 200, with an automated gain control (AGC) target value of 1.0 × 106, and a maximum ion injection of 120 ms. Differentially expressed proteins (DEPs) from MCI+ and AD+ samples were defined as those with a fold change greater than 1.5 and with a P-value less than 0.01, compared with those from CU samples.

A gene ontology (GO) search was performed to explore the biological processes related to the differentially expressed tear fluid proteins associated with MCI+ and AD+ groups. GO biological processes (GOBP) enriched by DEPs were identified as those with a P-value less than 0.01. We collected protein-protein interaction (PPI) from the STRING public database to construct a network depicting the enrichment processes. The network model was built with sorted DEPs and interactome data using Cytoscape.

4. Individual tear fluid analysis and data processing

For individual tear fluid analysis, parallel reaction monitoring (PRM) was performed using an LC-MS platform. We spiked 1 pmol of beta-galactosidase peptide as an internal standard in trypsin digestion step across samples. First, non-labeled pooled tear peptides were analyzed by single shot runs to confirm exact retention time of quantifiable DEPs in PRM mode with 80 min run time. One microgram of sample was injected into the LC-MS/MS system, and the PRM assay was set in the time-scheduled acquisition mode with a retention time +/− 3 min and resolution of 17,500 (AGC target to 1e5, maximum injection time of 100 ms). The chromatographic peak width was 30 s with NCE at 35%, and an isolation window of 1.6 m/z. Skyline software (version 19.1.0.193) was used for relative quantification in the PRM. Statistical analyses were carried out using Metaboanlyst 4.0 web-based software for principal component analysis (PCA) and hierarchical clustering with heat mapping.

5. Acquisition and analysis of PET and MR images

Using a Biograph mCT PET/computed tomography (CT) scanner (Siemens Medical Solutions, Malvern, PA, USA), we acquired PET images for 20 minutes, 80 minutes after the injection of ^{18}F-flortaucipir, and 90 minutes after the injection of ^{18}F-florbetaben. The two PET scans were done on separate days. CT images were acquired for attenuation correction prior to the PET scan. Finally, 3D PET images were reconstructed in a 256 × 256 × 223 matrix with 1.591 × 1.591 × 1 mm voxel size using the ordered-subsets expectation maximization algorithm. Axial T1-weighted brain MR images were acquired using a 3.0 Tesla MR scanner (Discovery MR750; GE Medical Systems, Milwaukee, WI, USA) with 3D-spoiled gradient-recalled sequences (512 × 512 matrix with voxel spacing 0.43 × 0.43 × 1 mm voxel size). T1-weighted MR images were processed with FreeSurfer 5.3 (Massachusetts General Hospital) software and participant-specific volume-of-interest (VOI) mask images were created following the same process as described in our previous study.[14] MR images were first resliced to FreeSurfer space, 25 segmented into gray and white matter. The 3D-surfaces for gray and white matter were then reconstructed. Cortical regions were parcellated using curvature information, and subcortical regions were segmented using the probabilistic registration method. Participant-specific composite VOI images for 20 cortical and subcortical regions were created by merging anatomically related regions. Voxel counts for each region were considered as the regional volume.

Statistical parametric mapping 12 (Wellcome Trust Centre for Neuroimaging, London, UK) and in-house software implemented in

MATLAB R2017b (MathWorks, Natick, MA, USA) were used to process the PET images and measure regional uptake values. PET images were co-registered to individual MR images within FreeSurfer space, and then partial volume effect (PVE) was corrected with the region-based voxel-wise method by using the participant-specific VOI images.[15] PVE-corrected standardized uptake value ratio (SUVR) images were then created with the cerebellar crus median obtained by overlaying the template cerebellar crus VOI on the spatially normalized PET images. Finally, we measured regional PVE-corrected SUVR values by overlaying the participant-specific composite VOIs. Regional meta-regions of interest were calculated using the voxel-number weighted average of median uptake. The lateral temporal meta-region of interest included the superior, middle, and inferior temporal cortices; the medial temporal meta-region of interest included the entorhinal, hippocampus, parahippocampus, amygdala, and insular cortices; the parietal meta-region of interest included the superior and inferior parietal cortices; and the cingulate meta-region of interest included the anterior and posterior cingulate cortices.

6. Statistical analysis

Statistical analysis was performed using SPSS 23 software (IBM Corp., Armonk, NY, USA). Two-sample *t*-tests were used for group comparisons, and chi-square tests were used for continuous and categorical demographic data. A stepwise method was performed to select variables to generate the receiver operating characteristic (ROC) curves and the AUCs. Youden's method was used to identify the optimal cut-off point on the ROC curves. Age,

sex, and duration of education were corrected for the adjusted model using SAS software (version 9.4; SAS Institute, Inc., Cary, NC, USA). The correlation analysis of imaging biomarkers used MR images and ^{18}F-florbetaben PET scans from 80 participants [17 CU, 27 MCI+, and 36 AD+] and ^{18}F-flortaucipir PET from 44 participants [11 CU, 14 MCI+, and 19 AD+]. Pearson's correlation was performed to test association between the tear fluid biomarkers and regional SUVRs and cortical volume. Region-wise multiple comparisons were corrected using the Benjamin-Hochberg's false-discovery rate method.[16] Medcalc 17.2 (MedCalc Software, Ostend, Belgium), and GraphPad Prism 7 (GraphPad software, San Diego, CA, USA) software was used for analysis and visualization of data.

III. RESULTS

Table 1 summarizes the demographic characteristics of the participants. In the global profiling cohort, patients with MCI+ and AD+ were older than CU individuals, and patients with AD+ showed a higher frequency of APOE ε4 genotype than CU individuals. In the individual analysis cohorts, patients in the AD+ group had a shorter duration of education, lower Mini-Mental State Examination (MMSE) scores, and higher Clinical Dementia Rating Sum-of-Box (CDR-SB) scores compared to the MCI+ and CU groups.

Table 1. Baseline demographic characteristics and clinical characteristics

	CU	MCI+	AD+
Global profiling cohort			
N	12	15	15
Age (years)	66.9±8.5	74.9±7.9*	76.9±8.8*
Sex (M:F)	3:9	9:6	4:11
Education (years)	12.5±4.1	12.1±4.6	8.8±5.5
APOE ε4+ (ε4+:ε4-)	1:8 (N/A 3)	5:9 (N/A 1)	8:7*
MMSE	28.4±2.2	24.5±2.9	17.7±5.8*†
CDR	0.3±0.2	0.8±0.5	1.3±0.8*
CDR-SB	0.6±0.5	3.1±2.8*	7.6±4.2*†
Individual analysis cohort			
N	30	32	41
Age (years)	70.5±9.7	73.6±8.3	74.6±9.2
Sex (M:F)	11:19	17:15	14:27
Education (years)	11.6±4.8	13.4±4.6	10.3±5.3*†
APOE ε4+ (ε4+:ε4-)	4:22 (N/A 4)	12:16 (N/A 4)	24:16 (N/A 1)
MMSE	27.8±1.6	25.6±2.8	19.2±5.1*†
CDR	0.4±0.2	0.5±0.1	0.8±0.4*†
CDR-SB	0.8±1.0	1.8±1.2	5.1±2.7*†

Data are presented as mean ± standard deviation.

*$P < 0.05$ for the comparisons between CU and each group. †$P < 0.05$ for the comparisons between MCI+ and AD+ groups.

Abbreviations: CU = cognitively unimpaired; MCI+ = amyloid-β-positive mild cognitive impairment; AD+ = amyloid-β-positive Alzheimer's disease; APOE = apolipoprotein E; MMSE = Mini-Mental State Examination; CDR-SB = Clinical Dementia Rating sum-of-boxes; N/A = not available

We detected 3,350 proteins in tear fluid from the global profiling cohort (Figure 2A and 2B). The identified tear proteome was estimated to cover a

dynamic range of approximately nine orders of magnitude (Figure 2C), demonstrating high proteome coverage. These quantitative global profiling results showed reproducibility in hierarchical clustering and correlation analysis (Appendix Figure 1). The largest portion of the cellular components of tear proteins were related to vesicle, extracellular, and cytosol proteins (Appendix Figure 2).

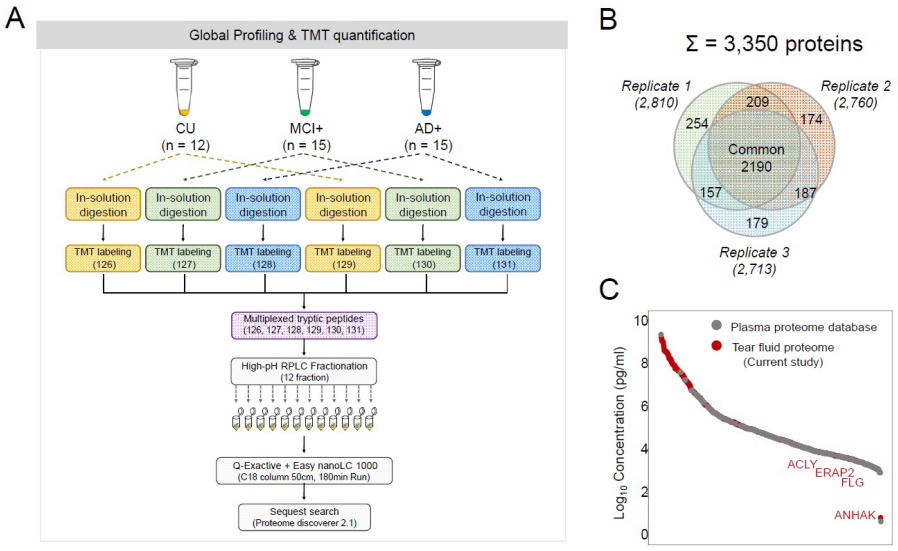

Figure 2. Global profiling of proteome using tandem-mass-tag (TMT) labeling. (A) Schematic representation of comprehensive tear proteome profiling including TMT labeling, high-pH reverse phase fractionation, and liquid chromatography-mass spectrometry/mass spectrometry (LC−MS/MS) analysis. (B) A diagram describing our approach for identifying total tear proteins in triplicate. (C) Distribution of the protein concentration of

identified tear fluid proteins with the reference plasma proteins. Protein concentration estimates were obtained from the Plasma Proteome Database.
Abbreviations: CU = amyloid-β-negative cognitively unimpaired; MCI+ = amyloid-β-positive mild cognitive impairment; AD+ = amyloid-β-positive Alzheimer's disease

Of the total proteins, 127 DEPs were identified from the MCI+ group tear fluid samples, 16 were downregulated and 111 were upregulated compared to the CU samples. Furthermore, 727 DEPs were identified from AD+ group tear fluid samples; 23 were downregulated and 704 were upregulated, compared to the CU samples (Figure 3A). The top five GOBP-enriched proteins in tear samples from the MCI+ and AD+ groups were similar (Figure 3B). In patients with either MCI+ or AD+, tear proteins were associated with the mRNA metabolic process, immune system, and transport, indicating the interconnection of their underlying biological processes (Figure 3C and 3D).

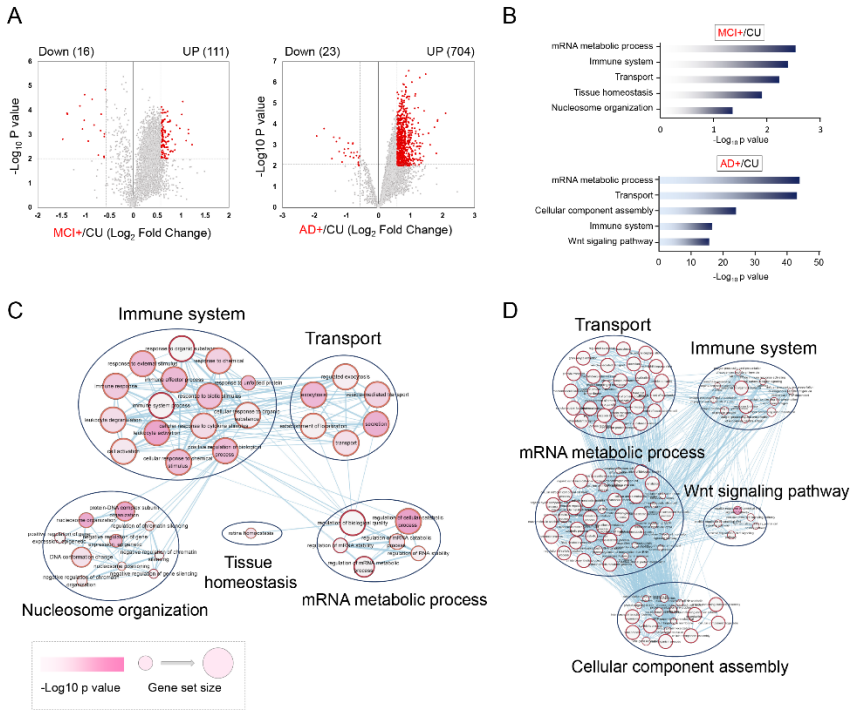

Figure 3. Altered proteins in the global proteome. (A) Volcano plot depicting the variance of tear proteome expression in the Aβ-positive mild cognitive impairment (MCI+) and Aβ-positive Alzheimer's disease (AD+) groups compared to the cognitively unimpaired (CU) group. Differentially expressed proteins (DEPs; *P*-value < 0.01 and fold change > 1.5) are indicated with red dots. (B) Gene Ontology biological process (GOBP) terms of DEPs in tear fluid samples from MCI+ and AD+ groups (top 5). The network of the representative GOBP network and reactome pathway analysis using DEPs in tear fluid samples from (C) MCI+ and (D) AD+ groups, structured by EnrichmentMap and Autoannoate in Cytoscape. Nodes are colored by -Log_{10} (*P*-value) and sized based on the number of genes.

Abbreviations: CU = amyloid-β-negative cognitively unimpaired; MCI+ = amyloid-β-positive mild cognitive impairment; AD+ = amyloid-β-positive Alzheimer's disease

Next, we verified specific biomarkers in our individual analysis cohort using the PRM-MS method. We identified 71 proteins which were quantifiable within the volume of individual samples of tear fluid collected at a single time (Figure 4A, and Appendix Figure 3). In Figure 4B, the score plot with the first two principal components shows 68.4% variance in tear proteome profiles. PCA demonstrated that there was a prominent separation between groups: MCI+ showed more similarities with AD+ than with CU. Of these 71 proteins, 22 tear biomarkers were common with the list of proteins identified by TMT-MS analysis, and eight biomarkers were common with DEPs of AD+ and MCI+ identified by TMT-MS. These were shown to be biologically connected as depicted in the PPI network, and were involved in transport and immune system processes (Figure 4C). A heat map depicting hierarchical clustering of these eight biomarkers also shows distinct intensities of in the AD+ and MCI+ groups, compared to the CU group (Figure 4D).

The fold change and AUC for biomarker candidates between diagnostic groups are shown in table 2. Secretoglobin family 2A member 1 (SCGB2A1) indicated a trend of increased expression related with the AD progression (CU < MCI+ < AD+). LCP1 showed a trend of decreased expression related with AD progression (table 2). All biomarkers differentiated CU from Aβ-positive cognitively impaired (CI+) with AUCs ranging from 0.654 to 0.874, and

differentiated CU from MCI+ with AUCs ranging from 0.655 to 0.876. All biomarkers (LCN1, LCP1, PIP, SCGB2A1, SCGB1D1, and GLUL) differentiated AD+ from CU with AUCs ranging from 0.673 to 0.859. LCP1, PIP, and CAP1 differentiated MCI+ from AD+ with AUCs ranging from 0.627 to 0.757.

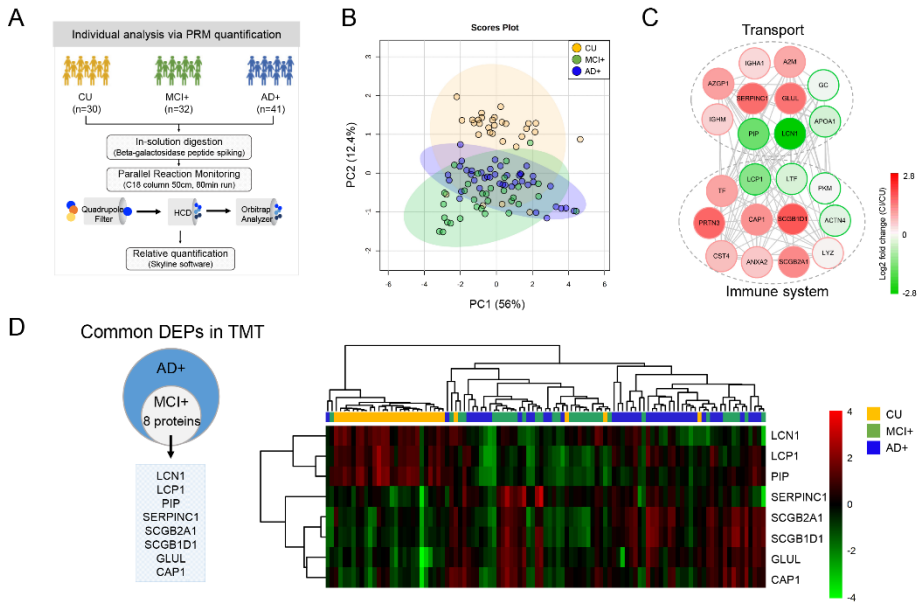

Figure 4. Individual tear fluid analysis using PRM analysis. (A) Overall workflow of the parallel reaction monitoring (PRM) assay for investigating candidate biomarkers of tear fluid in the Aβ-positive mild cognitive impairment (MCI+) and Aβ-positive Alzheimer's disease (AD+) groups compared to the cognitively unimpaired (CU) group. (B) Principal component analysis showing the difference in protein expression of tear fluid among the three groups. (C) Protein-protein interaction network of 22 differentially

expressed proteins (DEPs) identified by PRM. The amyloid-β-positive cognitively impaired (CI+) group was compared to the CU group, nodes are colored by $\log_2$ (fold change) with red indicating upregulation and green indicating downregulation. (D) Venn diagram determining eight PRM-targetable DEPs that also belonged to common DEPs in tandem-mass-tag mass (TMT) quantification (left panel). Hierarchical clustering and heat map indicating the intensities of eight candidate markers of tear fluid for AD or MCI (right panel).

Abbreviations: CU = amyloid-β-negative cognitively unimpaired; CI = amyloid-β-positive cognitively impaired; MCI+ = amyloid-β-positive mild cognitive impairment; AD+ = amyloid-β-positive Alzheimer's disease

Table 2. Eight candidate biomarkers of tear fluid for Alzheimer's disease and the diagnostic probability of each protein according to disease progression.

	Fold change			Areas under the curve			
Gene name	CI+/CU	MCI+/CU	AD+/CU	CU vs CI+	CU vs AD+	CU vs MCI+	MCI+ vs AD+
LCN1	0.14	0.14	0.14	0.853†	0.856†	0.856†	0.547
LCP1	0.42	0.51	0.36	0.774†	0.859†	0.774†	0.627*
PIP	0.33	0.19	0.43	0.874†	0.741†	0.876†	0.689*
CAP1	2.24	3.30	1.42	0.825†	0.620	0.828†	0.757†
SERPIN	3.02	4.88	1.56	0.716†	0.627	0.715†	0.608
SCGB2A	2.40	2.32	2.46	0.654*	0.673†	0.655*	0.541
SCGB1D	3.59	4.45	2.92	0.704†	0.719†	0.703†	0.567
GLUL	2.86	3.48	2.37	0.806†	0.773†	0.807†	0.574

$^{*}P < 0.05$, $^{\dagger}P < 0.01$ for comparison between groups.

Abbreviations: CU = cognitively unimpaired; MCI+ = amyloid-β-positive mild cognitive impairment; AD+ = amyloid-β-positive Alzheimer's disease; CI+ = amyloid-β-positive cognitively impaired; LCN1 = lipocalin 1; LCP1 = plastin-2; PIP = prolactin-inducible protein; CAP1= adenylyl cyclase-associated protein 1; SERPINC1 = serpin Family C Member 1; SCGB2A1 = secretoglobin family 2A member 1; SCGB1D1 = secretoglobin family 1D Member 1; GLUL = glutamine synthetase

We performed multiple regression analyses using various parameter combinations of eight tear proteins to obtain the best diagnostic power of tear biomarkers for differentiating between CU and CI+, and between MCI+ and AD+. The best biomarker combination was SERPINC1, PIP, LCP1, and GLUL, generating models with an AUC > 0.9 for discrimination of each diagnostic group, as shown in Figure 4. Moreover, the model adjusted for sex, age, and duration of education showed that the combination of LCP1 and CAP1 reached an AUC > 0.8 for discrimination of each diagnostic group (Figure 5).

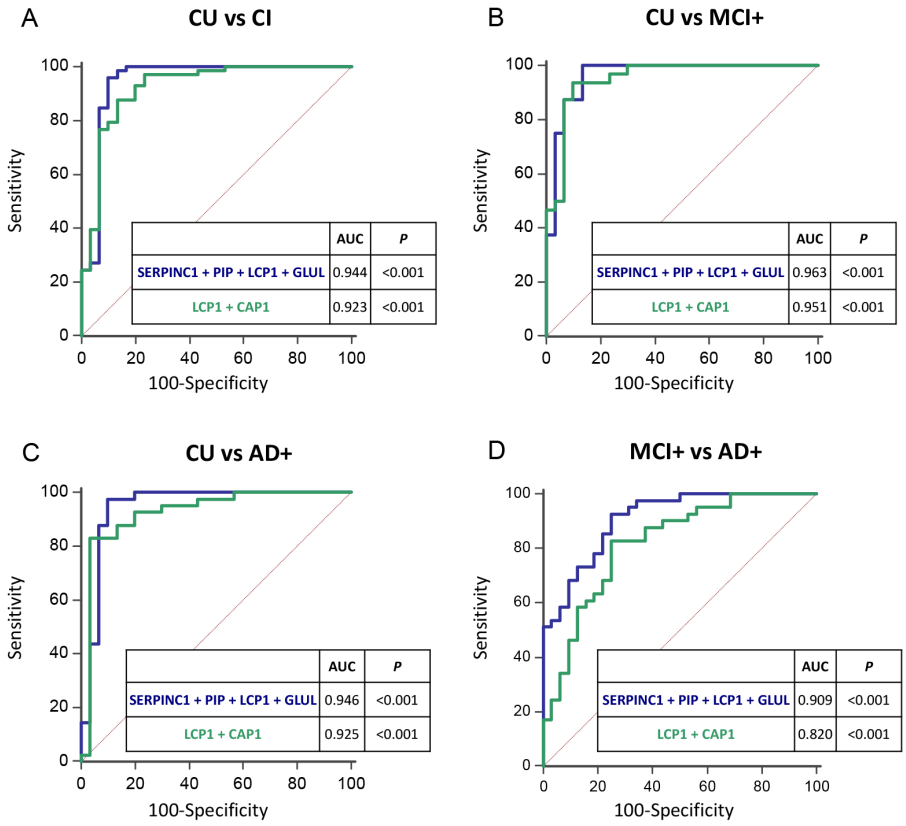

Figure 5. Receiver operating characteristic (ROC) curves of composite tear fluid biomarkers. ROC curves for diagnosis of (A) Aβ-positive CI, (B) MCI+, (C) AD+ and (D) an ROC curve between MCI+ and AD+.

Abbreviations: CU = amyloid-β-negative cognitively unimpaired; CI = amyloid-β-positive cognitively impaired; MCI+ = amyloid-β-positive mild cognitive impairment; AD+ = amyloid-β-positive Alzheimer's disease; AUC = area under curve; LCN1 = lipocalin 1; LCP1 = plastin-2; PIP = prolactin-inducible protein; CAP1 = adenylyl cyclase-associated protein 1; SERPINC1 = serpin Family C Member 1; GLUL = glutamine synthetase

We next confirmed the correlation of the tear fluid biomarker candidates with Aβ, tau, and cortical volume. LCN1 and LCP1 showed a negative association with Aβ burden in the diffuse cortical regions including the frontal, sensorimotor, medial and lateral temporal, parieto-occipital, precuneus, and cingulate cortices. Increased glutamine synthetase (GLUL) was associated with greater Aβ burden in the cingulate cortex (Figure 6). LCN1 was negatively associated with tau burden in the medial temporal cortex, and LCP1 was negatively associated with tau burden in the parietal, occipital, and lateral and medial temporal cortices (Figure 6). Only LCN1 was associated with cortical volume in the parietal and temporal regions (Figure 6). Representative cases showing the relationship between tear fluid biomarker levels and neuroimaging biomarkers are presented in the appendix (Appendix Figure 4).

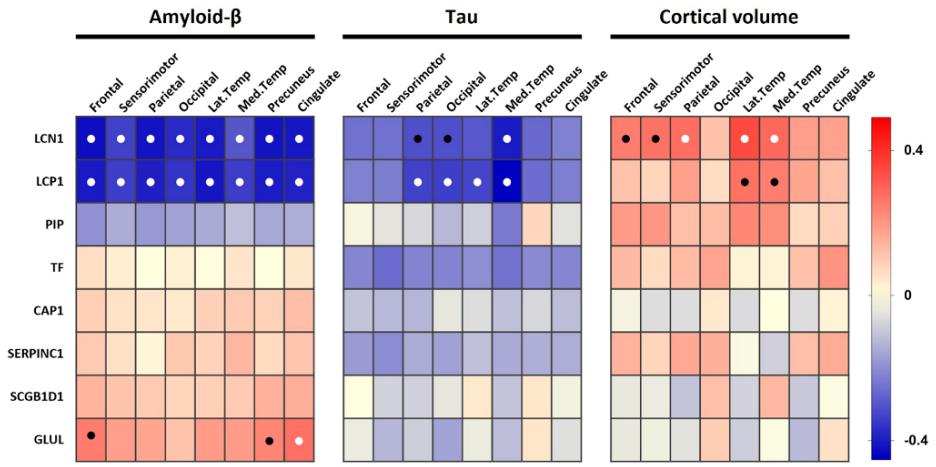

Figure 6. Heatmap correlations between tear fluid biomarkers and regional amyloid-β, tau burden, and cortical volumes. White dots represent significant correlation (*P*-value < 0.05) after Bonferroni's correction for multiple comparisons. Black dots indicate regions which did not survive multiple comparisons.

Abbreviations: LCN1 = lipocalin 1; LCP1 = plastin-2; PIP = prolactin-inducible protein; CAP1 = adenylyl cyclase-associated protein 1; SERPINC1 = serpin Family C Member 1; SCGB2A1 = secretoglobin family 2A member 1; SCGB1D1 = secretoglobin family 1D Member 1; GLUL = glutamine synthetase

IV. DISCUSSION

In this study, we found biomarkers in the human tear fluid of patients with Aβ-positive MCI and AD through proteome data from a global profiling

cohort as well as from an individual analysis cohort. The biomarkers were detectable from within a small number of individual tear samples. The diagnostic model using tear biomarkers effectively discriminated between Aβ-negative and Aβ-positive individuals, and also discriminated between MCI and AD in the Aβ-positive cohort, reflecting an association between the selected tear proteins and the clinical severity of AD. Furthermore, we determined that a subset of tear proteins showed a strong correlation with neuroimaging biomarkers in AD.

Previous studies have established AD-related alterations in the ocular system and a relationship between LG and AD pathology.[7] A recent radiology study reported an intense uptake of ^{18}F-florbetapir within human LG.[17] The abnormal function of cholinergic neurons that innervate the LG along the trigeminal nerve may be associated with changes in the protein composition of tear fluid in AD.[18]

Despite the advantages of using tear fluid proteins such as the non-invasive and affordable nature of testing and the relationship between tear fluid and the central nervous system, to the best of our knowledge, only two studies have been conducted to assess tear biomarkers in AD. One study using LC-MS/MS with in-gel digestion (excised band) suggested LCN1, lacritin, dermcidin, and lysozyme-C as tear fluid biomarkers for AD.[7] A more recent study used LC-MS/MS with in-gel digestion (stacking gel) to find 12 proteins with incremental changes with AD progression.[19] However, the sample size of the previous studies were relatively small. In comparison, our study had a large sample size (n=47 with AD and n=57 with MCI) with confirmation of Aβ

positivity as well as correlation with tau burden and cortical volume in AD spectrum.

Using global proteome profiling with TMT quantification, we identified a large number of tear proteins. Compared to previous studies,[9, 20] 1,884 additional proteins were identified in tear fluid. Our TMT approach provided a comprehensive list of DEPs found in tear fluid samples from patients with MCI+ and AD+, thus extensively extending the current list of candidate biomarkers previously identified by conventional small-scale approaches. Our data also confirmed the previously reported DEPs in tear fluid with AD. The list of proteins provided by our study is expected to serve as a comprehensive resource for the study of AD. Furthermore, TMT-based global protein profiling and PRM-based proteomics provide high resolution and more accurate quantification. Using a combination of the expression levels of GLUL, SERPINC1, PIP, and LCP1, our statistical model showed high diagnostic function not only in discriminating CU and Aβ+ cognitively impaired individuals (AUC = 0.944), but also in discriminating patients with MCI+ and AD+ (AUC = 0.909), thus enabling indication of disease severity. The results of our model showed improved accuracy compared to previous studies using tear fluid and blood.[21] Evaluation of longitudinal changes of neuroimaging biomarkers or cognitive function among CU individuals with different levels of tear proteins would clarify the temporal consequence of the changes in the levels of tear proteins and AD pathologies and clinical progression.

Glutamine synthetase, encoded by the GLUL gene localized in astrocytes, protects neurons by converting potentially neurotoxic glutamate and ammonia

into glutamine. Postmortem studies have shown an increase in the co-localization of reactive astrocytes with amyloid plaques as AD progresses.[22] The level of glutamine synthetase is increased in the CSF of patients with AD.[23] In the current study, the increased level of GLUL in tear fluid of MCI+ and AD+ groups concurs with previous studies and may reflect amyloidosis in AD.

Plastin-2 encoded by the LCP1 gene is a microglial and astrocytic protein marker. Microglial and astrocytic proteins, including LCP1, have greater expression in AD, and have been associated with Aβ and tau burden in a postmortem study.[24] LCN1 levels are reported to be decreased in the tear fluid of patients with AD.[7] Lipocalin-1 encoded by the LCN1 gene belongs to a family of small secretory proteins. Lipocalins have an important role in the innate immune response to bacterial infection and inflammation.[25] While LCN1 has shown an association with AD in genome wide association studies,[26] its function related to the pathogenesis of AD remains unclear.

Antithrombin III, encoded by the SERPINC1 gene has an important role in the inhibition of serine proteases in the coagulation cascade. It can accelerate protease inhibition and has anti-inflammatory effects.[27] In a postmortem study, increased antithrombin III levels were associated with astrogliosis and neurofibrillary pathology in AD.[28] Moreover, SERPINC1 gene expression was increased in the choroid plexus epithelium of patients with AD.[29] CAP1 controls actin filament turnover through recycling cofilin-1 and actin proteins. Interestingly, CAP1 knockdown results in the aggregation and dephosphorylation of cofilin-1 in cells, and the levels of cofilin aggregates are increased four-fold in patients with AD.[30]

Due to the exploratory nature of our study with a moderate sample size, our findings should be interpreted with caution and need confirmation using larger longitudinal studies. Nevertheless, we have performed in-depth proteome profiling in patients with Aβ-positive MCI and AD, and identified novel potential biomarkers that may indicate the perturbation of molecular pathways implicated in AD pathogenesis.

V. CONCLUSION

Tear fluid provides an easily assessable biomarker for the diagnosis of AD. Evaluation of alteration in tear protein profile may enable large-scale population screening and monitoring of disease progression in patients with MCI and AD.

REFERENCES

1. Zetterberg H, Blennow K. Plasma Abeta in Alzheimer's disease--up or down? *Lancet Neurol* 2006;5:638-639.

2. Ingelsson M, Fukumoto H, Newell KL, Growdon JH, Hedley-Whyte ET, Frosch MP, et al. Early Abeta accumulation and progressive synaptic loss, gliosis, and tangle formation in AD brain. *Neurology* 2004;62:925-931.

3. Wong MW, Braidy N, Poljak A, Pickford R, Thambisetty M, Sachdev PS. Dysregulation of lipids in Alzheimer's disease and their role as potential biomarkers. *Alzheimers Dement* 2017;13:810-827.

4. Knopman DS, Siemers ER, Bain LJ, Hendrix JA, Carrillo MC. National Institute on Aging - Alzheimer's Association Research Framework lays the groundwork for deeper understanding of Alzheimer's disease. *Alzheimers Dement* 2018;14:261-262.

5. Jessen F. Refining the understanding of typical Alzheimer disease. *Nat Rev Neurol* 2019;15:623-624.

6. Omar SH, Preddy J. Advantages and Pitfalls in Fluid Biomarkers for Diagnosis of Alzheimer's Disease. *J Pers Med* 2020;10.

7. Kallo G, Emri M, Varga Z, Ujhelyi B, Tozser J, Csutak A, et al. Changes in the Chemical Barrier Composition of Tears in Alzheimer's Disease Reveal Potential Tear Diagnostic Biomarkers. *PLoS One* 2016;11:e0158000.

8. Zhou L, Beuerman RW. The power of tears: how tear proteomics research could revolutionize the clinic. *Expert Rev Proteomics* 2017;14:189-191.

9. Jung JH, Ji YW, Hwang HS, Oh JW, Kim HC, Lee HK, et al. Proteomic analysis of human lacrimal and tear fluid in dry eye disease. *Sci Rep* 2017;7:13363.

10. Rossi C, Cicalini I, Cufaro MC, Agnifili L, Mastropasqua L, Lanuti P, et al. Multi-Omics Approach for Studying Tears in Treatment-Naive Glaucoma Patients. *Int J Mol Sci* 2019;20.

11. Kuo MT, Fang PC, Chao TL, Chen A, Lai YH, Huang YT, et al. Tear Proteomics Approach to Monitoring Sjogren Syndrome or Dry Eye Disease. *Int J Mol Sci* 2019;20.

12. Jack CR, Jr., Bennett DA, Blennow K, Carrillo MC, Dunn B, Haeberlein SB, et al. NIA-AA Research Framework: Toward a biological definition of Alzheimer's disease. *Alzheimers Dement* 2018;14:535-562.

13. Villemagne VL, Ong K, Mulligan RS, Holl G, Pejoska S, Jones G, et al. Amyloid imaging with (18)F-florbetaben in Alzheimer disease and other dementias. *J Nucl Med* 2011;52:1210-1217.

14. Cho H, Choi JY, Hwang MS, Kim YJ, Lee HM, Lee HS, et al. In vivo cortical spreading pattern of tau and amyloid in the Alzheimer disease spectrum. *Ann Neurol* 2016;80:247-258.

15. Thomas BA, Erlandsson K, Modat M, Thurfjell L, Vandenberghe R, Ourselin S, et al. The importance of appropriate partial volume correction for PET quantification in Alzheimer's disease. *Eur J Nucl Med Mol Imaging* 2011;38:1104-1119.

16. Benjamini Y, Hochberg Y. Controlling the False Discovery Rate - a Practical and Powerful Approach to Multiple Testing. *Journal of the Royal Statistical Society Series B-Statistical Methodology* 1995;57:289-300.

17. Itani M, Gunes BY, Akaike G, Behnia F. Lacrimal gland uptake on F-18 florbetapir amyloid positron emission tomography scan. *Radiol Case Rep* 2018;13:265-268.

18. Clader JW, Wang Y. Muscarinic receptor agonists and antagonists in the treatment of Alzheimer's disease. *Curr Pharm Des* 2005;11:3353-3361.

19. Kenny A, Jimenez-Mateos EM, Zea-Sevilla MA, Rabano A, Gili-Manzanaro P, Prehn JHM, et al. Proteins and microRNAs are differentially expressed in tear fluid from patients with Alzheimer's disease. *Sci Rep* 2019;9:15437.

20. Kishazi E, Dor M, Eperon S, Oberic A, Turck N, Hamedani M. Differential profiling of lacrimal cytokines in patients suffering from thyroid-associated orbitopathy. *Sci Rep* 2018;8:10792.

21. Kang S, Jeong H, Baek JH, Lee SJ, Han SH, Cho HJ, et al. PiB-PET Imaging-Based Serum Proteome Profiles Predict Mild Cognitive Impairment and Alzheimer's Disease. *J Alzheimers Dis* 2016;53:1563-1576.

22. Vehmas AK, Kawas CH, Stewart WF, Troncoso JC. Immune reactive cells in senile plaques and cognitive decline in Alzheimer’s disease. *Neurobiol Aging* 2003;24:321-331.

23. Tumani H, Shen G, Peter JB, Bruck W. Glutamine synthetase in cerebrospinal fluid, serum, and brain: a diagnostic marker for Alzheimer disease? *Arch Neurol* 1999;56:1241-1246.

24. Seyfried NT, Dammer EB, Swarup V, Nandakumar D, Duong DM, Yin L, et al. A Multi-network Approach Identifies Protein-Specific Co-expression in Asymptomatic and Symptomatic Alzheimer's Disease. *Cell Syst* 2017;4:60-72 e64.

25. Sia AK, Allred BE, Raymond KN. Siderocalins: Siderophore binding proteins evolved for primary pathogen host defense. *Curr Opin Chem Biol* 2013;17:150-157.

26. Rouillard AD, Gundersen GW, Fernandez NF, Wang Z, Monteiro CD, McDermott MG, et al. The harmonizome: a collection of processed datasets gathered to serve and mine knowledge about genes and proteins. *Database* 2016;1:1-16.

27. Lu ZY, Wang F, Liang MY. SerpinC1/Antithrombin III in kidney-related diseases. *Clinical Science* 2017;131:823-831.

28. Kalaria RN, Golde T, Kroon SN, Perry G. Serine protease inhibitor antithrombin III and its messenger RNA in the pathogenesis of Alzheimer's disease. *Am J Pathol* 1993;143:886-893.

29. Bergen AA, Kaing S, ten Brink JB, Netherlands Brain B, Gorgels TG, Janssen SF. Gene expression and functional annotation of human choroid plexus epithelium failure in Alzheimer's disease. *BMC Genomics* 2015;16:956.

30. Rahman T, Davies DS, Tannenberg RK, Fok S, Shepherd C, Dodd PR, et al. Cofilin rods and aggregates concur with tau pathology and the development of Alzheimer's disease. *J Alzheimers Dis* 2014;42:1443-1460.

APPENDICES

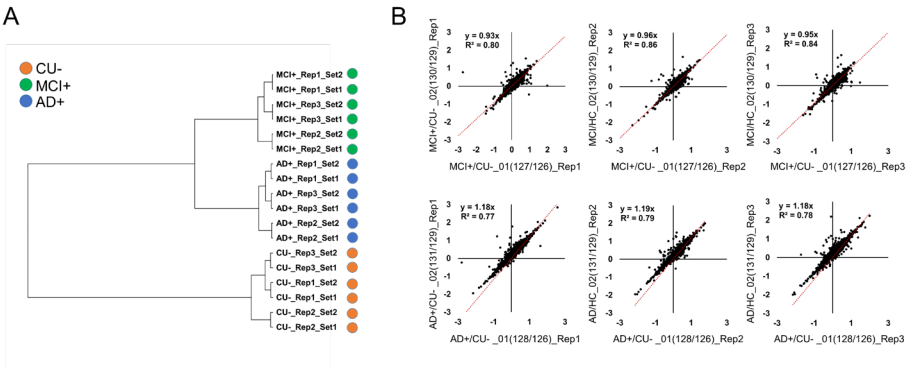

Appendix Figure 1. Reproducibility of global profiling of proteome. (A) Dendrogram showing hierarchical clustering of groups according to tear proteome data obtained from three instrumental replicates (Rep 1, 2, 3) and two tandem-mass-tag (TMT)-technical replicates (Set 1, 2). (B) Technical replicate correlations by ratio of intensity exported from TMT reporter ions, which show good reproducibility for two TMT sets (TMT-126, 129 : CU-, TMT-127, 130 : MCI+, TMT-128, 131 : AD+)

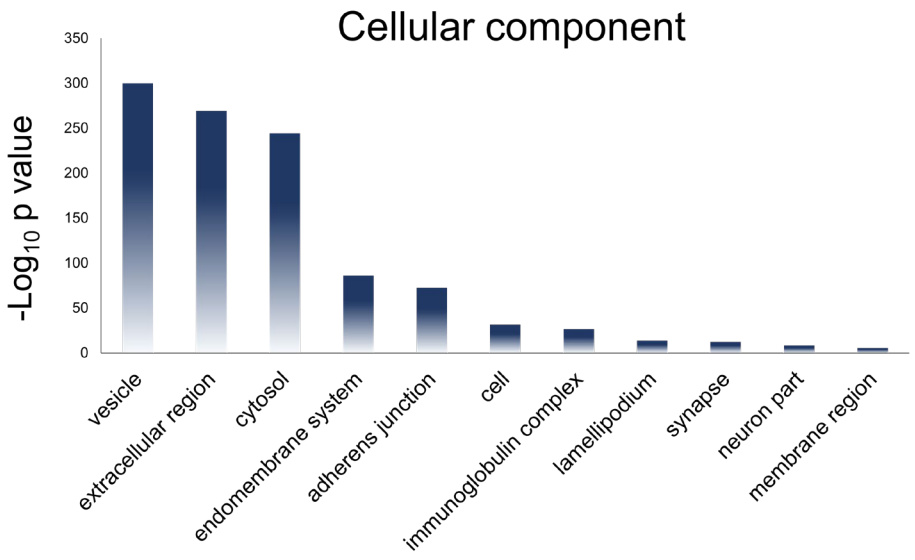

Appendix Figure 2. Identified gene ontology of cellular components of tear proteome.

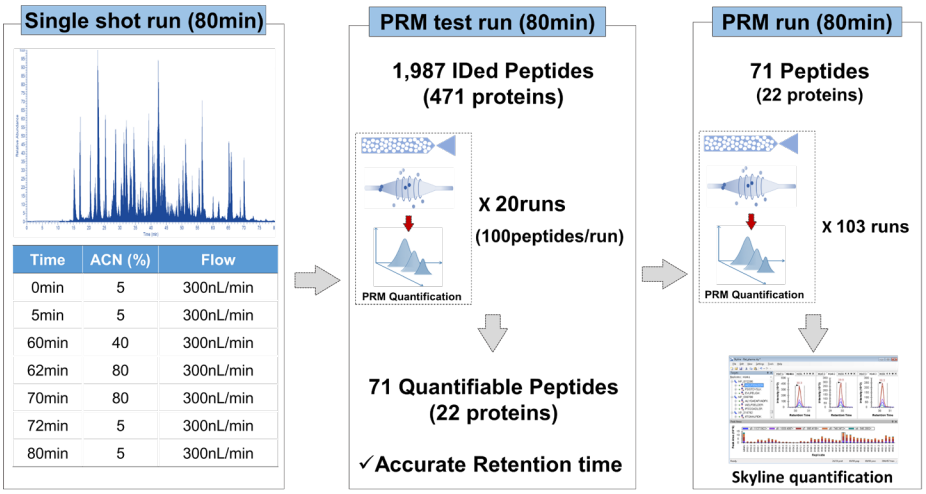

Appendix Figure 3. Workflow of proteomic analysis for parallel reaction monitoring (PRM). An retention time of peptides was confirmed by single shot run (80 min). PRM analysis using 71 transition peptides followed by peak area extraction using Skyline software.

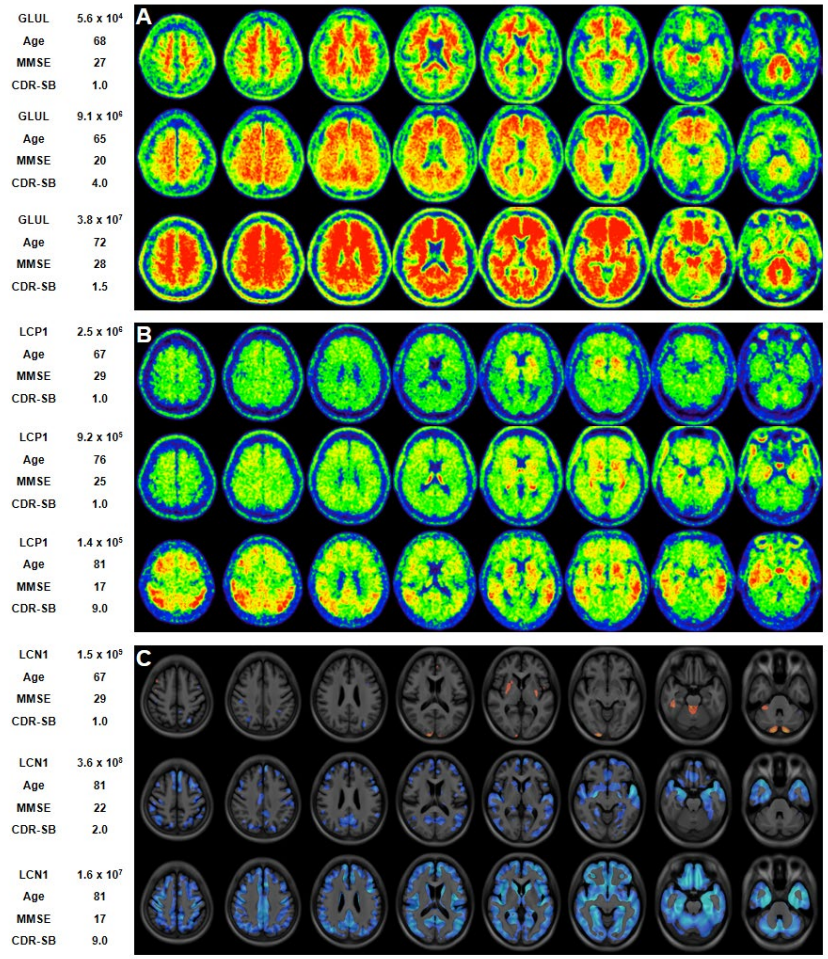

Appendix Figure 4. Representative PET and MR images showing the correlation between neuroimaging biomarkers and tear fluid biomarkers. (A) amyloid-β, (B) tau, and (C) cortical volume in individuals with different expression of tear fluid biomarkers. Color scale for ^{18}F-florbetaben ranges from SUVR 0 to 3.0, for ^{18}F-flortaucipir from SUVR 0 to 2.5, and for cortical volume from Z-score 0 to 2.0 with reference to the data from CU individuals.

ABSTRACT (IN KOREAN)

눈물 검체를 이용한 알츠하이머병 진단 바이오마커

<지도교수 류 철 형>

연세대학교 대학원 의학과

백민석

배경: 알츠하이머병을 진단하기 위해 현재 뇌척수액검사와 양전자방출단층촬영술을 통한 바이오마커가 사용되고 있으나, 이 검사들은 침습적이거나 높은 비용의 문제로, 대규모의 환자를 대상으로 한 검사에는 제한점이 있다. 본 연구에서는 인간의 눈물검체를 이용하여 알츠하이머 치매와 경도인지장애 환자를 진단할 수 있는 바이오마커를 프로테오믹스 방법을 통하여 새롭게 발견하고자 하였다.

방법: 본 연구에서는 정상인지군, 아밀로이드-베타 양성 경도인지장애 환자, 아밀로이드-베타 양성 알츠하이머 치매 환자로

구성된 42명의 프로파일링 코호트에서 분광분석법을 통하여 새로운 눈물검체 바이오마커를 찾고, 103명으로 구성된 개인분석 코호트에서 이 바이오마커를 개별적으로 정량화 하였다. 로지스틱 회귀분석과 수신자 판단 특성 곡선 분석을 통하여 눈물검체 바이오마커의 진단 능력을 평가하고, 개인별 양전자방출단층 영상 및 뇌자기공명 영상에서 도출된 아밀로이드-베타, 타우 단백의 분포 및 뇌 회질의 부피가 눈물검체 바이오마커의 정량적 측정값과 가지는 상관관계를 분석하였다.

결과: 프로파일링 코호트에서 총 3,350개의 눈물 검체 단백질이 검출되었으며, 이 중 22개의 단백질이 개인분석에서 재확인 되었고, 최종적으로 8개의 눈물검체 바이오마커가 알츠하이머 치매의 진단에 통계적으로 유효한 결과를 보였다. 새롭게 발견된 눈물검체 바이오마커 중 lipocalin 1 (LCN1), plastin-2 (LCP1), prolactin-inducible protein (PIP), secretoglobin family 2A member 1 (SCGB2A1), secretoglobin family 1D Member 1 (SCGB1D1), glutamine synthetase (GLUL)는 인지정상군으로부터 아밀로이드-베타 양성 알츠하이머 치매 환자를 진단하는 데 있어 높은 진단 능력을 보였다 (Area Under the Curve, AUC 0.67 – 0.86). 또한 바이오마커의 조합을 통하여, 정상인지군, 아밀로이드-베타 양성 경도인지장애 환자, 아밀로이드-베타 양성 알츠하이머 치매 환자군을 각각 구분하는데 있어서 높은 진단 능력을 도출하였다.

(AUC >0.8). 바이오마커 중 GLUL은 뇌 회질의 아밀로이드-베타 축적정도와 양의 상관관계를 보였으며, LCN1과 LCP1은 아밀로이드-베타 및 타우의 축적정도와 음의 상관 관계를 보였다.

결론: 새롭게 발견된 눈물검체 바이오마커는 아밀로이드-베타 양성 경도인지장애 및 아밀로이드-베타 양상 알츠하이머 치매 환자를 효율적으로 진단할 뿐만 아니라, 알츠하이머병의 병리학적소견을 반영하고 있어, 비침습적이고 경제적인 알츠하이머병 진단 도구가 될 수 있을 것으로 생각된다.

핵심되는 말: 알츠하이머병, 경도인지장애, 눈물 검체, 생체표지자

PUBLICATION LIST

1. Baek MS, Cho H, Lee HS, Choi JY, Lee JH, Ryu YH, et al. Temporal trajectories of in vivo tau and amyloid-beta accumulation in Alzheimer's disease. *Eur J Nucl Med Mol Imaging* 2020;47:2879-2886.

2. Baek MS, Cho H, Lee HS, Lee JH, Ryu YH, Lyoo CH. Effect of A/T/N imaging biomarkers on impaired odor identification in Alzheimer's disease. *Sci Rep* 2020;10:11556.

3. Baek MS, Cho H, Lee HS, Lee JH, Ryu YH, Lyoo CH. Effect of APOE epsilon4 genotype on amyloid-beta and tau accumulation in Alzheimer's disease. *Alzheimers Res Ther* 2020;12:140.

4. Baek MS, Cho H, Ryu YH, Lyoo CH. Customized FreeSurfer-based brain atlas for diffeomorphic anatomical registration through exponentiated lie algebra tool. *Ann Nucl Med* 2020;34:280-288.

5. Cho H, Baek MS, Lee HS, Lee JH, Ryu YH, Lyoo CH. Principal components of tau positron emission tomography and longitudinal tau accumulation in Alzheimer's disease. *Alzheimers Res Ther* 2020;12:114.

6. Baek MS, Han K, Kwon H-S, Lee Y-h, Cho H, Lyoo CH. Risks and Prognoses of Alzheimer's Disease and Vascular Dementia in Patients With Insomnia: A Nationwide Population-Based Study. *Frontiers in Neurology* 2021;12.

7. Baek MS, Lee MJ, Kim HK, Lyoo CH. Temporal trajectory of biofluid markers in Parkinson's disease. *Sci Rep* 2021;11:14820.